Ferromagnetic Exchange Coupling and Magneto-Structural Correlations in Mixed-Bridged Trinuclear Copper(II) Complexes. Magnetic Data and Theoretical Investigations and Crystal Structures of Two Angled Cu^{II}_3 Complexes

Stefan Gehring,* Peter Fleischhauer, Helmut Paulus,† and Wolfgang Haase

Institut für Physikalische Chemie, Technische Hochschule Darmstadt, D-6100 Darmstadt, FRG

Received September 24, 1991

The structural and magnetic data of two angled trinuclear compounds, $[Cu^{II}_3(2\text{-}CH_3C_6H_4CO_2)_4\{(C_2H_5)_2NC_2H_4O\}_2H_2O]$, **3**, and $[Cu^{II}_3(C_6H_5CO_2)_4\{(C_2H_5)_2NC_2H_4O\}_2H_2O]$, **6**, are reported. Crystal data: for **3**, space group $C2/c$, $a = 27.726$ (5) Å, $b = 20.190$ (4) Å, $c = 8.314(2)$ Å, $\beta = 101.08$ (1)°, $Z = 4$; for **6**, space group $C2/c$, $a = 14.549$ (5) Å, $b = 12.456$ (4) Å, $c = 24.368$ (8) Å, $\beta = 90.14$ (1)°, $Z = 4$. Both complexes show similar molecular structures with an isosceles triangular Cu_3 unit and the central Cu(2) on the C_2 axis. The Cu(1) and Cu(2) coordination spheres are square pyramidal with H_2O as a common apical ligand. The mixed bridging by an aminoethanolato oxygen atom and a bidentate carboxylato group leads to a noncoplanarity of adjacent basal copper coordination planes with dihedral angles $\varphi_{AB} = 66.8°$ (**3**) and 66.6° (**6**). The isosceles structures are compared to the linear analogues of the series $[Cu^{II}_3(RC_6H_4CO_2)_4(R'_2NC_2H_4O)_2(R''OH)_n]$ (R', R'' = alkyl; $n = 2$). Structural correlations are presented, and the role of hydrogen-bond bridging is discussed. Susceptibility measurements (4.2-290 K) reveal ferromagnetic exchange coupling in the mixed-bridged moiety Cu(II)-RO/RCO_2-Cu(II) leading to a quartet ground state for **3** and **6**. Fit parameters are as follows: for **3**, $J_{12} = 26.8$ (10.0), $J_{13} = 0$ cm^{-1}, $g = 2.18$ (0.06), $\Theta = -0.1$ (0.5) K; for **6**, $J_{12} = 26.6$ (5.0), $J_{13} = 0$ cm, $g = 2.11$ (0.03), $\Theta = -1.5$ (0.5) K ($\hat{H} = -2\sum_{j>i=1} J_{ij}S_iS_j$). The ferromagnetic exchange coupling is discussed using SCF-Cl calculations on model compounds. A summary of the theoretical results for the mixed-bridged unit Cu(II)-RO/RCO_2-Cu(II) is given including calculated magneto-structural correlations as functions $2J_{calcd}$ vs φ_{AB}. The singly occupied molecular orbitals used for the construction of magnetic orbitals are analyzed. The experimental magneto-structural data for the series $[Cu^{II}_3(RC_6H_4CO_2)_4(R'_2NC_2H_4O)_2(R''OH)_n]$ agree with the theoretical results.

Introduction

The actual studies on exchange-coupled systems are governed at least by two topics, the research for molecular ferromagnets[1,2] and the magnetic characterization of polynuclear active sites in metalloproteins.[3,4] Trinuclear copper(II) systems with (dialkylamino)ethanolato/benzoato bridging, $[Cu_3(RC_6H_4CO_2)_4(R'_2NC_2H_4O)_2(R''OH)_n]$, are of interest for both areas:

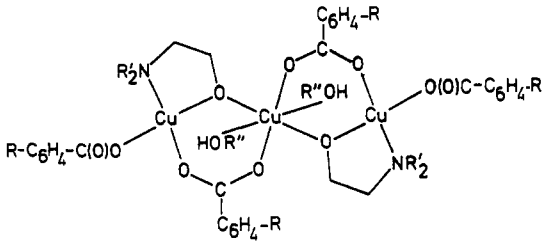

The ferromagnetic exchange coupling in the mixed-bridged unit Cu(II)-RO/RCO_2-Cu(II) leads to a quartet ground state for the trinuclear system,[5-7] which is uncommon within trinuclear copper(II) complexes investigated so far.[5,8,9] The magneto-structural studies on this mixed-bridged moiety[10] may be useful in the design of molecular-based ferromagnetic materials.

In various metalloproteins, also, mixed bridging of the metal centers is found, e.g. in hemerythrin the unit Fe(III)-O/$(RCO_2)_2$-Fe(III)[11] and in ribonucleotide reductase the unit Fe(III)-O/(RCO_2)-Fe(III).[12] For oxyhemocyanin an active site having a core of Cu(II)-RO/O_2-Cu(II) is postulated.[13] Therefore investigations on mixed-bridged systems are helpful for a better understanding of the magnetic properties of biomolecules. Increasing interest in trinuclear copper systems has been stimulated by the investigations on laccase[14] and ascorbate oxidase.[15] Magnetic circular dichroism studies of laccase[14a,b] confirmed a

† Present address: Fachgebiet Strukturforschung, Fachbereich Materialwissenschaft, TH Darmstadt, Darmstadt, FRG.

(1) Proceedings of the International Conference on Molecular Based Magnetic Materials. *Mol. Cryst. Liq. Cryst.* **1989**, *176*.
(2) *Magnetic Molecular Materials*; Gatteschi, D., Kahn, O., Miller, J. S., Palacio, F., Eds.; NATO ASI Series 198; Kluwer Academic Publishers: Dordrecht, The Netherlands, 1991.
(3) Fifth International Conference on Bioinorganic Chemistry. *J. Inorg. Biochem.* **1991**, *43*.
(4) *Metal Clusters in Proteins*; Que, L., Jr., Ed.; ACS Symposium Series 372; American Chemical Society: Washington, DC, 1988.
(5) Haase, W.; Gehring, S. *J. Chem. Soc., Dalton Trans.* **1985**, 2609.
(6) Gehring, S.; Astheimer, H.; Haase, W. *J. Chem. Soc., Faraday, Trans. 2* **1987**, *83*, 347.
(7) Gehring, S.; Paulus, H.; Haase, W.; Bill, E.; Trautwein, A. X. *Z. Kristallogr.* **1990**, *186*, 83.
(8) Chaudhuri, P.; Winter, M.; Della Védova, B. P. C.; Bill, E.; Trautwein, A. X.; Gehring, S.; Fleischhauer, P.; Nuber, B.; Weiss, J. *Inorg. Chem.* **1991**, *30*, 2148.
(9) (a) References in refs. 5 and 8. (b) Comarmond, J.; Dietrich, B.; Lehn, J.-M.; Louis, R. *J. Chem. Soc., Chem. Commun.* **1985**, 74. (c) Journaux, Y.; Sletten, J.; Kahn, O. *Inorg. Chem.* **1986**, *25*, 439. (d) Costes, J.-P.; Dahan, F.; Laurent, J.-P. *Inorg. Chem.* **1986**, *25*, 413. (e) Epstein, J. M.; Figgis, B. N.; White, A. H.; Willis, A. C. *J. Chem. Soc., Dalton Trans.* **1974**, 1954. (f) Chiari, B.; Piovesana, O.; Tarantelli, T.; Zanazzi, P. F. *Inorg. Chem.* **1985**, *24*, 4615. (g) Muhonen, H.; Hatfield, W. E. *Acta Chem. Scand.* **1986**, *A40*, 41. (h) Halvorson, K. E.; Grigereit, T. E.; Willett, R. D. *Inorg. Chem.* **1987**, *26*, 1719. (i) Grigereit, T. E.; Ramakrishna, B. L.; Place, H.; Willett, R. D.; Pellacani, G. C.; Manfredini, T.; Menabue, L.; Bonamartini-Corradi, A.; Battaglia, L. P. *Inorg. Chem.* **1987**, *26*, 2235. (j) Bensch, W.; Seferiadis, H.; Oswald, H. R. *Inorg. Chim. Acta* **1987**, *126*, 113.
(10) Gehring, S.; Haase, W. *Mol. Cryst. Liq. Cryst.* **1989**, *176*, 513.
(11) Stenkamp, R. E.; Sieker, L. C.; Jensen, L. H. *J. Am. Chem. Soc.* **1984**, *106*, 618.
(12) Nordlund, P.; Sjöberg, B.-M.; Eklund, H. *Nature* **1990**, *345*, 593.
(13) Salvato, B.; Beltramini, M. *Life Chem. Rep.* **1990**, *8*, 1.
(14) (a) Allendorf, M. D.; Spira, D. J.; Solomon, E. I. *Proc. Nat. Acad. Sci. USA* **1985**, 3063. (b) Spira-Solomon, D. J.; Allendorf, M. D.; Solomon, E. I. *J. Am. Chem. Soc.* **1986**, *108*, 5318. (c) Cole, J. L.; Tan, G. O.; Yang, E. K.; Hodgson, K. O.; Solomon, E. I. *J. Am. Chem. Soc.* **1990**, *112*, 2243.

0020-1669/93/1332-0054$04.00/0

Table I. Trinuclear Compounds $[Cu_3(RC_6H_4CO_2)_4(R'_2NC_2H_4O)_2(R''OH)_n]$

	R	R′	R″	n	ref
1	H	C_2H_5	CH_3	2	5
2	H	n-C_4H_9	C_2H_5	2	5, 16
3	2-CH_3	C_2H_5	H	1	7, 17; this work
4	3-CH_3	C_2H_5	CH_3	2	7, 17, 18
5A, 5B[a]	4-CH_3	n-C_4H_9	CH_3	2	7, 17, 19
6	H	C_2H_5	H	1	this work

[a] Two crystallographically independent linear trinuclear molecules in the asymmetric unit.

trinuclear active site which consists of a mononuclear type 2 and a dinuclear type 3 cupric center. The X-ray structure of ascorbate oxidase[15a] revealed an angled Cu_3 arrangement with an approximate C_2 symmetry and copper–copper separations of 3.4 Å within the type 3 center and of about 4 Å within the type 2 center.

With this contribution, we continue our reports on mixed-bridged trinuclear copper complexes of the general formula $[Cu_3(RC_6H_4CO_2)_4(R'_2NC_2H_4O)_2(R''OH)_n]$. The structurally and magnetically investigated compounds are summarized in Table I. In this series of ferromagnetically exchange coupled copper(II) trimers the linear Cu_3 arrangement with $D_{\infty h}$ symmetry was found in **1**, **2**, **4**, and **5**. One part of this work deals with the magnetic and structural properties of the compounds **3** and **6**. They are—as far as known—the first compounds with an isosceles triangular Cu_3 unit (symmetry C_{2v}) exhibiting quartet spin ground states. In the angled trinuclear copper(II) complexes hitherto investigated magnetically[8,9a–e] doublet spin ground states were found due to antiferromagnetic coupling. The Cu–Cu–Cu angles vary between 97 and 156°.[9e]

A knowledge of the magnetic and structural properties of **3** and **6** allows an analysis of some interesting properties of the series of trinuclear copper(II) complexes with quartet spin ground states. Ferromagnetic exchange coupling and properties of the magnetic orbitals are discussed on the basis of SCF–Cl calculations reported recently.[6,10,17] Therefore, only a short summary of the theoretical results is given. Structural and magneto–structural correlations for **1**–**6** are presented and compared to the theoretical data. Studies dealing with EPR investigations on the spin ground states[19] and excited states[20] are in progress.

Experimental Section

Syntheses. 3. A 505-mg amount (4.31 mmol) of (diethylamino)-ethanol in 1 mL of methanol was added to a suspension of 715 mg (2.14 mmol) of copper(II) 2-methylbenzoate in 5 mL of methanol at 50 °C.[18] After a few days at ambient temperature blue needle-shaped crystals suitable for X-ray studies separated from the turquoise green solution. Anal. Calcd for $C_{44}H_{58}Cu_3N_2O_{11}$ (**3**): C, 53.84; H, 5.96; N, 2.85. Found: C, 53.74; H, 5.94; N, 2.81.

6. The trinuclear complex **1**[5] was dissolved in dichloromethane and the solvent evaporated at ambient temperature. Addition of acetone and slow evaporation led to X-ray-suitable blue prismatic single crystals. Anal. Calcd for $C_{40}H_{50}Cu_3N_2O_{11}$ (**6**): C, 51.91; H, 5.45; N, 3.03. Found: C, 51.78; H, 5.47; N, 3.10.

Crystal Structure Determinations. Intensity data of single crystals of **3** and **6** were collected on four-circle diffractometers with graphite-(002)-monochromated Mo Kα radiation in the scan mode $\omega:2\theta = 1:1$ ("learnt profile"). Details of the crystal data determinations and intensity data treatments are summarized in Table II. Standard intensities showed no evidence for crystal decay. The data were corrected for Lorentz and polarization effects, and a numerical absorption correction (SHELX76[21]) was applied. Both structures were solved by direct methods with SHELX86[22] and refined with SHELX76. The scattering factors for Cu^0 were taken from ref 23; other were used as stored in the programs. All non-hydrogen atoms were refined anisotropically; carbon-bound hydrogen atoms were positioned as geometrically idealized with C–H = 0.96 Å and $U_{iso}(H) \approx U_{eq}$ of the corresponding carbon atom. The hydrogen atom of the water molecule in **6**, H(O6), was localized in a difference-Fourier map and included in the refinement. In case of **3** the hydrogen atom H(O6) could not be localized. The comparatively high residual electron density in **3** associated with $R = 0.10$ may be attributed to the quality of the investigated crystal. Final atomic coordinates and equivalent temperature factors are given in Tables III and IV.

Table II. Crystallographic Data for **3** and **6**

	3	**6**
chem formula	$C_{44}H_{58}Cu_3N_2O_{11}$	$C_{40}H_{50}Cu_3N_2O_{11}$
a/Å	27.726 (5)	14.549 (5)
b/Å	20.190 (4)	12.456 (4)
c/Å	8.314 (2)	24.368 (8)
β/deg	101.08 (1)	90.14 (1)
V/Å^3	4567.3	4416.0
Z	4	4
fw	981.58	925.47
space group	$C2/c$ (No. 15)	$C2/c$ (No. 15)
T/°C	24	21
λ/Å (Mo Kα)	0.710 73	0.710 69
ρ_{calcd}/g cm^{-3}	1.427	1.392
μ(Mo Kα)/mm^{-1}	1.379	1.424
R, R_w[a]	0.1004, 0.0925	0.0418, 0.0385

[a] $R = \sum\|\|F_o\| - |F_c\|\|/\sum|F_o|$; $R_w = \sum(\|\|F_o\| - |F_c\|w^{1/2})/\sum(|F_o|w^{1/2})$, $w = k/(\sigma(F_o))^2$, k from least-squares refinement.

Table III. Atomic Coordinates and Equivalent Temperature Factors for **3**

atom	x	y	z	U_{eq}[a]
Cu(1)	0.0890 (1)	0.2429 (1)	0.7281 (2)	38 (1)
Cu(2)	0.0	0.1588 (1)	0.75	36 (1)
O(1)	0.0521 (2)	0.1670 (4)	0.626 (1)	36 (4)
O(2)	0.1120 (3)	0.1921 (5)	0.929 (2)	62 (6)
O(3)	0.0473 (3)	0.1314 (5)	0.945 (1)	51 (5)
O(4)	0.1219 (3)	0.3192 (4)	0.840 (1)	45 (5)
O(5)	0.0631 (3)	0.3358 (5)	0.982 (2)	70 (7)
O(6)	0.0	0.2770 (6)	0.75	41 (6)
N(1)	0.0934 (3)	0.2700 (6)	0.497 (2)	50 (7)
C(1)	0.0418 (5)	0.1729 (7)	0.451 (2)	49 (8)
C(2)	0.0844 (4)	0.2164 (9)	0.394 (2)	66 (10)
C(3)	0.0918 (5)	0.1450 (6)	0.985 (2)	42 (7)
C(4)	0.1239 (4)	0.1035 (6)	1.112 (2)	34 (6)
C(5)	0.1712 (4)	0.1277 (8)	1.180 (2)	54 (8)
C(6)	0.2012 (6)	0.0914 (9)	1.296 (3)	86 (12)
C(7)	0.1867 (6)	0.0331 (10)	1.350 (3)	85 (12)
C(8)	0.1417 (6)	0.0082 (9)	1.288 (2)	78 (11)
C(9)	0.1085 (5)	0.0430 (7)	1.170 (2)	50 (8)
C(10)	0.1057 (5)	0.3445 (7)	0.960 (2)	51 (8)
C(11)	0.1379 (5)	0.3893 (6)	1.073 (2)	41 (7)
C(12)	0.1158 (6)	0.4416 (7)	1.144 (2)	60 (9)
C(13)	0.1432 (7)	0.4851 (9)	1.250 (3)	85 (12)
C(14)	0.1925 (7)	0.4762 (10)	1.294 (3)	93 (13)
C(15)	0.2150 (6)	0.4255 (9)	1.232 (3)	76 (11)
C(16)	0.1887 (5)	0.3809 (7)	1.119 (2)	57 (9)
C(18)	0.1420 (5)	0.2998 (9)	0.492 (2)	77 (11)
C(19)	0.1850 (6)	0.2570 (9)	0.573 (3)	90 (13)
C(22)	0.0552 (5)	0.3239 (8)	0.428 (2)	64 (10)
C(23)	0.0573 (5)	0.3886 (8)	0.510 (3)	71 (11)
C(26)	0.0594 (5)	0.0123 (8)	1.112 (3)	75 (10)
C(27)	0.2154 (6)	0.3267 (9)	1.047 (3)	96 (13)

[a] $U_{eq} = (10^3/3)\sum_i\sum_j U_{ij}\, a_i^* a_j^* (a_i a_j)/$Å^2.

(15) (a) Messerschmidt, A.; Rossi, A.; Ladenstein, R.; Huber, R.; Bolognesi, M.; Gatti, G.; Marchesini, A.; Petruzzelli, T.; Finazzi-Agro, A. *J. Mol. Biol.* **1989**, *206*, 513. (b) Cole, J. L.; Avigliano, L.; Morpurgo, L.; Solomon, E. I. *J. Am. Chem. Soc.* **1991**, *113*, 9080.
(16) Muhonen, H.; Pajunen, A.; Hämäläinen, R. *Acta Crystallogr.* **1980**, *B36*, 2790.
(17) Gehring, S. Thesis, Technische Hochschule Darmstadt, FRG, 1990.
(18) Gehring, S.; Paulus, H.; Haase, W. *Acta Crystallogr.* **1991**, *C47*, 1814.
(19) Gehring, S.; Fleischhauer, P.; Haase, W.; Bill, E.; Trautwein, A. X. Manuscript in preparation.
(20) Fleischhauer, P.; Gehring, S.; Haase, W.; Bill, E.; Trautwein, A. X.; Zanchini, C.; Gatteschi, D. Manuscript in preparation.
(21) Sheldrick, G. M. SHELX76. Program for Crystal Structure Determination. University of Cambridge, 1976.
(22) Sheldrick, G. M. *Acta Crystallogr.* **1990**, *A46*, 467.
(23) *International Tables for X-ray Crystallography*; Kynoch: Birmingham, England, 1974; Vol. 4.

Table IV. Atomic Coordinates and Equivalent Temperature Factors for **6**

atom	*x*	*y*	*z*	U_{eq}[a]
Cu(1)	0.15671 (5)	0.42415 (5)	0.78906 (5)	54 (1)
Cu(2)	0.0	0.5671 (1)	0.75	48 (1)
O(1)	0.1322 (2)	0.5501 (2)	0.7461 (1)	48 (2)
O(2)	0.1103 (2)	0.4897 (2)	0.8562 (1)	66 (2)
O(3)	0.0085 (2)	0.6095 (2)	0.8262 (1)	60 (2)
O(4)	0.1739 (2)	0.2922 (2)	0.8302 (1)	62 (3)
O(5)	0.0262 (2)	0.2462 (3)	0.8343 (1)	80 (3)
O(6)	0.0	0.3731 (3)	0.75	58 (3)
N(1)	0.2491 (3)	0.3817 (3)	0.7307 (2)	71 (3)
C(1)	0.1773 (3)	0.5421 (4)	0.6945 (2)	70 (3)
C(2)	0.2625 (5)	0.4813 (4)	0.7006 (2)	133 (6)
C(3)	0.0567 (3)	0.5668 (4)	0.8627 (2)	52 (3)
C(4)	0.0482 (3)	0.6120 (3)	0.9196 (2)	52 (3)
C(5)	0.1041 (4)	0.5740 (5)	0.9605 (2)	100 (4)
C(6)	0.0954 (4)	0.6147 (6)	1.0134 (2)	126 (5)
C(7)	0.0330 (14)	0.6929 (5)	1.0246 (2)	90 (4)
C(8)	−0.0218 (3)	0.7306 (4)	0.9844 (2)	73 (4)
C(9)	−0.0152 (3)	0.6908 (4)	0.9317 (2)	63 (3)
C(10)	0.1069 (4)	0.2382 (4)	0.8486 (2)	58 (3)
C(11)	0.1308 (3)	0.1582 (3)	0.8925 (2)	52 (3)
C(12)	0.0714 (3)	0.0750 (4)	0.9034 (2)	70 (3)
C(13)	0.0909 (5)	−0.0004 (4)	0.9441 (2)	92 (5)
C(14)	0.1703 (5)	0.0102 (5)	0.9735 (3)	103 (5)
C(15)	0.2304 (4)	0.0940 (5)	0.9635 (2)	90 (4)
C(16)	0.2101 (3)	0.1667 (4)	0.9226 (2)	66 (3)
C(18)	0.2117 (4)	0.2905 (5)	0.6996 (2)	99 (5)
C(19)	0.2642 (6)	0.2490 (6)	0.6517 (3)	150 (7)
C(22)	0.3407 (5)	0.3477 (6)	0.7556 (3)	126 (7)
C(23)	0.3727 (6)	0.4044 (7)	0.8022 (3)	173 (10)

[a] See footnote *a* in Table III.

Magnetic Susceptibility Measurements. $\chi(T)$ data of powdered samples of **3** were recorded with a Faraday-type magnetometer[24] in the temperature range 4.2–290 K. For the measurement of **6** an improved system was used (computer-controlled Cahn D-200 microbalance, Bruker B-MN 200/60 power supply). Corrections of the experimental data for underlying diamagnetism[25] were calculated as -178×10^{-6} for **3** and -163×10^{-6} cm^3 mol^{-1} (per Cu) for **6**. Magnetic moments were obtained from $\mu_{eff}/\mu_B = 2.828\ (\chi T)^{1/2}$.

Calculations. Structure calculations, $\chi(T)$ fits, and theoretical calculations were performed on the IBM 3090-200E VF computer of the TH Darmstadt. Details of the SCF–CI calculations on model compounds were reported previously.[10,26]

Results and Discussion

Molecular Structures. Figure 1 presents the molecular structure of **3**, and Figure 2a shows the Cu_3 skeleton with coordinating atoms and bridges as found in **6**. Selected distances, bond angles, and dihedral angles are given in Table V.

Both compounds show the same principle structure, an isosceles triangular Cu_3 unit with the central Cu(2) on the 2-fold axis. The Cu(1)–Cu(2) distances are 3.030 (2) (**3**) and 3.044 (1) Å (**6**); the Cu(1)–Cu(2)–Cu(1)* angles are 111.2 (2)° (**3**) and 108.4 (1)° (**6**) (symmetry code (indicated by an asterisk): $-x, y, 1.5 - z$). The water oxygen atom O(6), positioned also on the C_2 axis, occupies the apical positions of the square pyramidal coordinations of the terminal Cu(1) and Cu(1)* centers as well as of the central Cu(2). The basal plane of the Cu(1) pyramid is formed by O(1), O(2), O(4), and N(1) (plane A), and that of Cu(2), by O(1), O(3), O(1)*, and O(3)* (plane B). Neighboring copper centers are bridged by the aminoethanolato-oxygen O(1) and the three-atomic carboxylato-group O(2)–C(3)–O(3). Like in the linear compounds of this type (Figure 2b, compounds **1**, **2**, **4**, and **5**) the mixed bridging leads to a noncoplanarity of the basal planes A and B characterized by the dihedral angles φ_{AB} = 66.8° (**3**) and 66.6° (**6**). The water molecule is fixed in the hydrogen-bond system O(5)···O(6)···O(5)*, which may be also responsible for a strong phenyl/carboxylato twist in the monodentate benzoato ligand with φ_{Bzl} = 33.2° (**3**) and 20.4° (**6**). A comparison between **3** and the unsubstituted analogue **6** shows no significant influence of the 2-methyl substituent on the molecular structure.

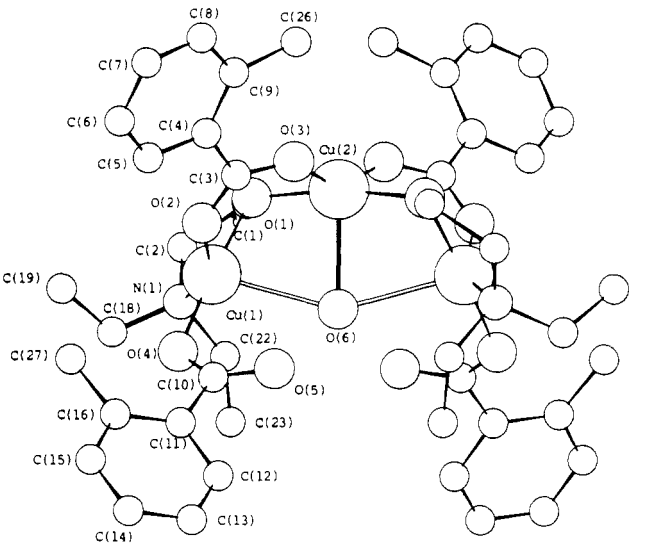

Figure 1. Molecular structure of **3**.

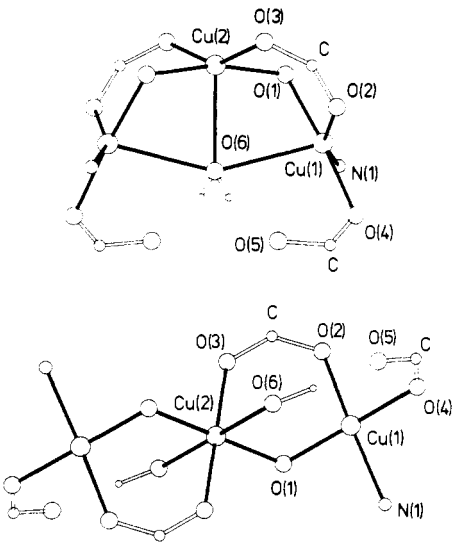

Figure 2. Cu_3 skeleton of **6** (a, top). For comparison a linear Cu_3 skeleton as found in **1**, **2**, **4**, and **5** is shown (b, bottom).

The knowledge of six structurally investigated compounds within the series of alkoxo/carboxylato-bridged trinuclear copper(II) complexes allows us to summarize some structural correlations. The coordination of one water molecule in the angled trinuclear systems instead of two alcohol molecules in the linear systems may be the reason for the different Cu_3 geometries. The water molecule forms two hydrogen bond bridges to O(5) and O(5)* whereas the alcohol binds only one free oxygen O(5) of the two unidentate benzoate ligands. In both cases the ROH molecules stabilize the structures. Examples are **1** with a linear Cu_3 unit and the angled compound **6**, whose chemical compositions differ only on the coordinated "solvent molecules".

The mixed-bridged moieties Cu(1)–RO/RCO_2–Cu(2) retain their structural properties independent from the Cu_3 symmetry. In **1**, **2**, **4**, and **5** it was found that the trans-angle O(2)–Cu(1)–N(1) becomes smaller with shortened Cu(1)–O(6) distances.[17,18] This effect of an increased distortion of the basal plane A holds also for **3** and **6**. The other trans-angle O(1)–Cu(1)–

(24) Merz, L.; Haase, W. *J. Chem. Soc., Dalton Trans.* **1980**, *875*.
(25) Weiss, A.; Witte, H. *Magnetochemie*; Verlag Chemie: Weinheim, FRG, 1973.
(26) Astheimer, H.; Haase, W. *J. Chem. Phys.* **1986**, *85*, 1427 and references therein.

Table V. Selected Distances (Å), Angles (deg), and Dihedral Angles (deg)[a] for **3** and **6**

	3	6
	Distances	
Cu(1)–Cu(2)	3.030 (2)	3.044 (1)
Cu(1)–Cu(1)*	5.000 (4)	4.938 (2)
Cu(1)–O(1)	1.945 (8)	1.918 (3)
Cu(1)–O(2)	1.958 (9)	1.951 (3)
Cu(1)–O(4)	1.935 (8)	1.940 (3)
Cu(1)–N(1)	2.024 (11)	2.030 (3)
Cu(1)–O(6)	2.601 (3)	2.549 (1)
Cu(2)–O(1)	1.937 (7)	1.938 (3)
Cu(2)–O(3)	1.958 (8)	1.934 (3)
Cu(2)–O(6)	2.387 (11)	2.416 (4)
O(2)–C(3)	1.239 (14)	1.247 (5)
O(3)–C(3)	1.245 (14)	1.251 (5)
O(4)–C(10)	1.278 (16)	1.268 (5)
O(5)–C(10)	1.243 (16)	1.228 (5)
	Angles	
O(5)···O(6)	2.63 (2)	2.619 (7)
C(26)–C(26)*	3.50 (2)	
Cu(1)–Cu(2)–Cu(1)	111.2 (2)	108.4 (1)
Cu(1)–O(1)–Cu(2)	102.6 (4)	104.2 (1)
O(1)–Cu(1)–O(2)	90.9 (4)	92.9 (1)
O(2)–Cu(1)–O(4)	87.7 (4)	88.0 (1)
O(4)–Cu(1)–N(1)	97.7 (4)	93.3 (1)
O(1)–Cu(1)–N(1)	85.5 (4)	87.3 (1)
O(1)–Cu(1)–O(4)	175.6 (3)	176.0 (1)
O(2)–Cu(1)–N(1)	151.7 (5)	158.2 (2)
O(1)–Cu(1)–O(6)	79.2 (3)	80.5 (1)
O(2)–Cu(1)–O(6)	103.8 (3)	96.1 (1)
O(4)–Cu(1)–O(6)	97.0 (3)	95.5 (1)
O(6)–Cu(1)–N(1)	103.1 (3)	105.5 (1)
O(1)–Cu(2)–O(3)	90.8 (3)	90.9 (1)
O(1)–Cu(2)–O(6)	85.1 (2)	83.7 (1)
O(3)–Cu(2)–O(6)	106.4 (3)	105.9 (1)
O(1)*–Cu(2)–O(3)	91.9 (4)	92.6 (1)
O(1)–Cu(2)–O(1)*	170.2 (4)	167.5 (1)
O(3)–Cu(2)–O(3)*	147.3 (4)	148.3 (1)
Cu(1)–O(2)–C(3)	128.8 (9)	130.4 (3)
O(2)–C(3)–O(3)	124.4 (13)	125.8 (4)
Cu(2)–O(3)–C(3)	129.1 (9)	127.0 (3)
Cu(1)–O(4)–C(10)	119.4 (8)	122.3 (3)
O(4)–C(10)–O(5)	123.0 (13)	126.3 (4)
O(5)···O(6)···O(5)*	126 (2)	105.8 (5)
Cu(1)···O(6)···Cu(1)*	149.4 (5)	151.1 (2)
	Dihedral Angles	
φ_{AB}	66.8	66.6
φ_{CD}	105.4	109.4
$\varphi_{Bz1} = \varphi_{EF}$	33.2	20.4
$\varphi_{Bz2} = \varphi_{GH}$	11.7	5.2

[a] Definitions of planes and best planes are as follows: Plane A, O(1), O(2), O(4), N(1); plane B, O(1), O(1)*, O(3), O(3)*; plane C, Cu(1), Cu(2), O(2), O(3), C(3); plane D, Cu(1), Cu(2), O(1); plane E, O(4), O(5), C(10); plane F, C(11)–C(16); plane G, O(2), O(3); C(3); plane H, C(4)–C(9). An asterisk indicates the symmetry code $-x, y, 1.5 - z$.

O(4) remains constant at 176 ± 1° (Table V). The bridging angle Cu(1)–O(1)–Cu(2) and the distance Cu(1)–Cu(2) correlate with the dihedral angle φ_{AB} (Figure 3). An increased folding of this "butterfly structure"[27] is associated with a more acute bridging angle and a shorter copper–copper distance. The structural properties of **1–6** vary in a comparatively broad range. The dihedral angle φ_{AB} covers a range of 10°, from 57 to 67°. This change in φ_{AB} is associated with variations of Cu(1)–O(1)–Cu(2) in a range from 103 to 115° and changes of the Cu(1)–Cu(2) distance from 3.03 to 3.23 Å.

Magnetic Properties. The temperature dependencies of the effective magnetic moments of **3** and **6** are shown in Figure 4. At room temperature effective magnetic moments of 1.98 (3) (**3**) and 1.92 (3) μ_B/Cu (**6**) were observed. With decreasing temperature the $\mu_{eff}(T)$ functions increase and pass through

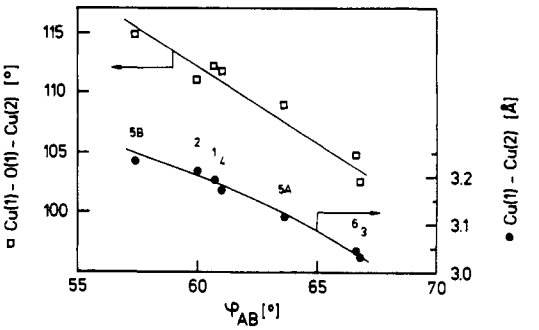

Figure 3. Structural correlation of the dihedral angle φ_{AB} with the bridging angle Cu(1)–O(1)–Cu(2) and the copper–copper distance Cu(1)–Cu(2) for **1–6**. The lines are drawn as a guide for the eye.

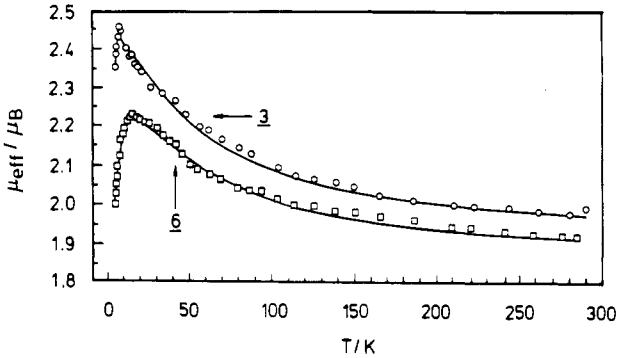

Figure 4. Magnetic moments (deg) vs temperature for **3** and **6**. The solid lines represent the fitted functions as described in the text.

maxima at 7 K, 2.50 (3) μ_B (**3**), and 14 K, 2.24 (3) μ_B (**6**). Such behavior is characteristic of predominant ferromagnetic exchange coupling in Cu^{II}_3 systems.[5]

As a basis for the interpretation of the magnetic data, we started from the isotropic Heisenberg–Hamiltonian for three paramagnetic centers in C_{2v} symmetry,[5,8]

$$\hat{H} = -2J_{12}(\hat{S}_1\hat{S}_2 + \hat{S}_2\hat{S}_3) - 2J_{13}(\hat{S}_1\hat{S}_3) \qquad (1)$$

with J_{12} as exchange coupling constant between the adjacent centers [in **3** and **6**: Cu(1)–Cu(2), Cu(2)–Cu(1)*] and J_{13} as coupling constant between the terminal centers [Cu(1)–Cu(1)*]. The resulting spin levels $|S_T = S_1 + S_2 + S_3, S^+ = S_1 + S_3\rangle$ for three interacting $S_i = {}^1/_2$ centers are one quartet, $|{}^3/_2, {}^1/_2\rangle$, and two doublets, $|{}^1/_2, 0\rangle$ and $|{}^1/_2, 1\rangle$, with energies $E(S_T,S^+)$ as $E({}^3/_2,1) = -J_{12} - J_{13}/2$, $E({}^1/_2,0) = 3J_{13}/2$, and $E({}^1/_2,1) = 2J_{12} - J_{13}/2$. Using the van Vleck equation, the following theoretical expression for the temperature dependence of χ is obtained:

$$\chi_{calcd}(T) = \frac{N_A g^2 \mu_B{}^2}{12k(T-\Theta)} \times \frac{10\exp(J_{12}/kT) + \exp(-2J_{12}/kT) + \exp(-2J_{13}/kT)}{2\exp(J_{12}/kT) + \exp(-2J_{12}/kT) + \exp(-2J_{13}/kT)} + N\alpha \qquad (2)$$

A Weiss Θ is included to describe phenomenologically the decrease of $\mu_{eff}(T)$ at low temperatures, which is caused by zero-field splitting effects of the quartet state and intercluster interactions.

The parameters obtained from nonlinear fits[28] of eq 2 to the experimental data are J_{12} = 26.8 (10.0) cm^{-1}, g = 2.18 (0.06), and Θ = –0.1 (0.5) K for **3** and J_{12} = 26.6 (5.0) cm, g = 2.11 (0.03), and Θ = –1.5 (0.5) K for **6**; J_{13} = 0 and $N\alpha = 60 \times 10^{-6}$ cm^3/mol^{-1} were both fixed. The function minimized was $R = \sum_n(\chi_{exp} - \chi_{calcd})^2T^2$, and the agreement factors $R_Q = (\sum_n|\chi_{exp} - \chi_{calcd}|/\chi_{exp})/n$ are 0.017 (**3**) and 0.008 (**6**). In Figure 4 the functions $\mu_{calcd}(T)$ are shown as solid lines. Fits with the terminal

(27) Fallon, G. D.; Murray, K. S.; Mazurek, W.; O'Connor, M. J. *Inorg. Chim. Acta* **1985**, *96*, L53.

(28) Olsson, D. M. *J. Qual. Technol.* **1974**, *6*, 53.

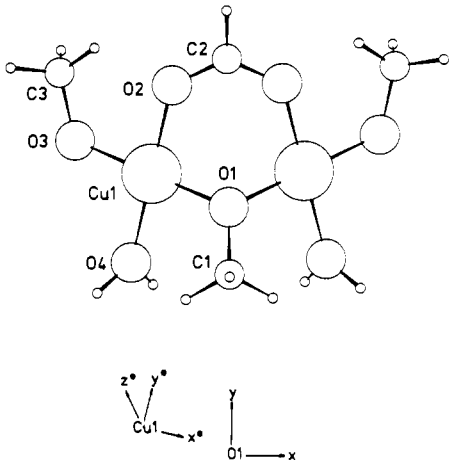

Figure 5. Model molecule M1 used for the SCF–CI calculations of the singlet–triplet splitting energy $2J_{calcd}$. The SCF–CI calculations were performed in the molecular orthogonal coordinate system x, y, z, with O1 as the origin. The local orthogonal coordinate system x^*, y^*, z^* with Cu1 as the origin is used for the discussion of atomic orbital contributions to the SOMO's.

coupling as a free fit parameter converged at $J_{13} \approx 0$ cm^{-1} and did not improve the quality of the fits. For **3** the exchange parameters change considerably when R_Q is used as a minimizing criterion; therefrom the greater error estimates result. As well, correlations between the $\chi(T)$ fit parameters are observed[17,29] when individual **g** tensors for the three spin multiplets are applied which are linear combinations of the single ion **g** tensors.[30]

Ferromagnetic coupling in the alkoxo/benzoato–bridged moieties leads to quartet ground states for both compounds. This is confirmed by the EPR spectra,[19] which show, around 4 K, transitions within the $m_s = \pm^1/_2$ Kramers' doublet of the quartet state. **3** shows an axial spectrum, and **6**, a rhombic one. The size and the sign of the J_{12} values of **3** and **6** agree as a result of the quite similar structural properties of the trinuclear cores. They agree also with the data found in the linear trinuclear systems **1**, **2**[5] and **4**, **5**.[17,19] The mechanism and magneto–structural correlations in this mixed-bridged system which results in ferromagnetic coupling will be discussed in more detail in the following section.

No influence on the exchange coupling between adjacent centers is found whether the Cu_3 unit is angled or linear. However, the coupling between the terminal centers is influenced. In the linear systems that have been studied it has been essential to include a nonzero J_{13} for the interpretation of the magnetic data;[5] e.g. in case of **5** $J_{13} = -15$ cm^{-1}.[19] Antiferromagnetic interactions between the terminal spin centers are established also in heterotrinuclear compounds. Examples with diamagnetic central metal ions are systems like Cu(II)–Ni^{LS}–Cu(II), Cu(II)–Pd(II)–Cu(II),[8] or Fe(III)–Fe(II)^{LS}–Fe(III);[31] an example with a paramagnetic central metal ion shows a Fe(III)–Cu(II)–Fe(III) core.[31] In **3** and **6** a possible pathway for a magnetic Cu(1)–Cu(1)* interaction is Cu(1)–O(6)–Cu(1)*. The magnetic orbitals centered on Cu(1) and Cu(1)* have predominantly $d_{x^{*2}-y^{*2}}$ character, referring to a local copper geometry in which the x^* and the y^* axes are defined by the Cu(1) basal plane (cf. Figure 5). A delocalization of the unpaired electron toward the apical ligand O(6) seems less pronounced due to the elongated Cu(1)–O(6) bond length. Single-crystal EPR studies[20] will be used to determine the degree of a dz^{*2} admixture into the Cu(1) ground state. Thus, on the basis of $\chi(T)$ data, a significant Cu(1)–Cu(1)* interaction via the O(6) oxygen atom can be excluded. Other pathways including the central Cu(2) coordination or the hydrogen-bond system O(5)···O(6)···O(5) do not seem suitable either, due to geometric properties like the noncoplanarity of the Cu(1)- and Cu(1)*-basal coordination planes. The problem of such "long-range interactions" is under discussion at least because of their relevance for biological systems.[32]

Ferromagnetic Exchange Coupling. Before discussing exchange coupling in mixed-bridged Cu(II)–RO/RCO$_2$–Cu(II) systems, we will summarize our results of SCF–CI calculations on model complexes.[6,10,17] Special attention is given to the atomic and molecular orbitals and structural effects leading to ferromagnetic coupling. The experimental results for **1–6** are compared to theoretically calculated magneto–structural correlations.

For the calculation of the singlet–triplet splitting ($2J_{calcd}$) in dinuclear copper(II) complexes, we used the method developed by de Loth et al.,[33] which has been successfully applied to a few systems recently.[26,33,34] $2J_{calcd}$ is obtained as a sum of terms arising in a CI treatment of localized magnetic orbitals a and b, which are defined by linear combinations of the symmetric and antisymmetric singly occupied molecular orbitals (SOMO's) from an open-shell SCF calculation. Molecules with symmetry C_i or C_s can be used. Details of this method are presented elsewhere.[26,33,34]

For our studies we constructed a C_s-symmetric dimeric model molecule M1 (Figure 5) from the crystal structure of the trinuclear compound **1**.[5] M1 reflects all structural properties of the mixed-bridged subunit as found in **1–6**, i.e. a butterfly structure with a dihedral angle $\varphi_{AB} = 71.3°$, Cu1–O1–Cu1 = 104.4°, and Cu1–O1 = 1.944 Å.[35] For the model compounds φ_{AB} is defined between the planes with atoms O1, O2, O3, O4 (plane A′) and O1, O2′, O3′, O4′. In the next step, effects of structural and electronic variations were studied by starting from the structure of M1. The dihedral angle was varied in the range $0° \le \varphi_{AB} \le 90°$ by rotating the plane A′ around the O1–O2 vector. The influence of the copper–oxygen distance r_{Cu-O} on the exchange coupling was studied between 1.79 and 2.09 Å, and the oxygen donor H_2O was replaced by the nitrogen donor NH_3 (O vs N).

The results of the SCF–CI calculation is shown in Figure 6 as $2J_{calcd}$ vs φ_{AB}. For folded structures, ferromagnetic exchange coupling via alkoxo/carboxylato bridges is confirmed. As planar geometry is approached, a singlet ground state is obtained depending on the Cu1–O1 bond length and the donor set (replacement of O vs N). Ferromagnetic spin coupling is nearly invariable in the region $\varphi_{AB} > 40°$. The parabolic functions can be fitted approximately to eq 3 with the parameters a_0, a_1, and

$$2J_{calcd}/\text{cm}^{-1} = a_2(\varphi_{AB}/\text{deg})^2 + a_1(\varphi_{AB}/\text{deg}) + a_0 \quad (3)$$

a_2 given in Table VI. The angle Cu–O–Cu′ covers a range 141–90° when φ_{AB} is changed from 0 to 90°. The structural change is associated with a variation in $2J_{calcd}$ of about |300| cm^{-1} with a crossover from antiferromagnetic to ferromagnetic coupling. In comparison with planar di-μ-alkoxo-bridged Cu_2O_2 systems the sensitivity of the singlet–triplet splitting toward structural

(29) (a) Banci, L.; Bencini, A.; Gatteschi, D. *Inorg. Chem.* **1983**, *22*, 2681. (b) Benelli, C.; Bunting, R. K.; Gatteschi, D.; Zanchini, C. *Inorg. Chem.* **1984**, *23*, 3074.
(30) *EPR of Exchanged Coupled Systems*; Bencini, A., Gatteschi, D., Eds.; Springer Verlag: Berlin, Heidelberg, Germany, 1990.
(31) Chaudhuri, P.; Winter, M.; Fleischhauer, P.; Haase, W.; Flörke, U.; Haupt, H.-J. *J. Chem. Soc., Chem. Commun.* **1990**, 1728.
(32) *Electron and Proton Transfer in Chemistry and Biology*; Müller, A., Diemann, E., Junge, W., Ratajczak, H., Eds.; Elsevier Publishers: Amsterdam, The Netherlands, 1991, in press.
(33) de Loth, P.; Cassoux, P.; Daudey, J.-P.; Mairieu, J. P. *J. Am. Chem. Soc.* **1981**, *103*, 4007.
(34) (a) Charlot, M. F.; Verdaguer, M.; Journaux, Y.; de Loth, P.; Daudey, J.-P. *Inorg. Chem.* **1984**, *23*, 3802. (b) de Loth, P.; Daudey, J.-P.; Astheimer, H.; Walz, L.; Haase, W. *J. Chem. Phys.* **1985**, *82*, 5048. (c) Nepveu, F.; Haase, W.; Astheimer, H. *J. Chem. Soc., Faraday Trans. 2* **1986**, *82*, 551. (d) Nepveu, F.; Gehring, S.; Walz, L. *Chem. Phys. Lett.* **1986**, *128*, 300. (e) de Loth, P.; Karafiloglou, P.; Daudey, J.-P.; Kahn, O. *J. Am. Chem. Soc.* **1988**, *110*, 5676.
(35) Atom labels of modeled molecules are given without parentheses to distinguish them from those referring to crystal structure data.

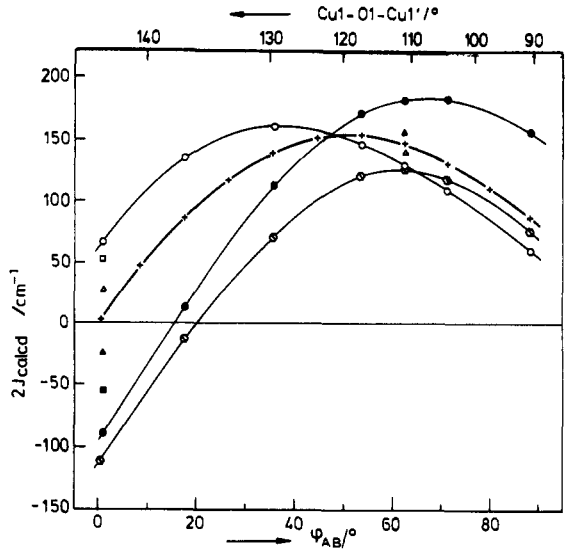

Figure 6. Calculated singlet–triplet splitting energies $2J_{calcd}$ vs φ_{AB} in dimeric copper(II) model molecules with alkoxo/carboxylato bridging. The Cu1–O1 distance (Å) was varied as 1.794 (●), 1.844 (■), 1.894 (▲), 1.944 (– + –), 1.994 (△), 2.044 (□), and 2.094 (○). The effect of the replacement of an O-donor (– + –) vs a N-donor (⊘) was calculated for Cu1–O1 = 1.944 Å. The Cu1–O1–Cu1′ angle is correlated to the dihedral angle φ_{AB}.[10] This is shown in the second x axis of the plot. For clarification the solid lines do not agree exactly with the fit data (eq 3; Table VI).

Table VI. Fit Parameters for $2J_{calcd}(\varphi_{AB})$ Functions and Calculated Maxima

	r_{Cu-O}/Å			
	1.794	1.944	2.094	1.944[a]
a_2 (cm^{-1}/(deg)^2)	–0.05845	–0.05540	–0.04824	–0.06490
a_1 (cm^{-1}/deg)	8.134	5.815	4.056	8.106
a_0 (cm^{-1})	–102.4	0.2	70.0	–132.0
$\varphi_{AB,max}$ (deg)	70	53	42	63
$2J_{calcd}(\varphi_{AB,max})$ (cm^{-1})	181	153	155	121

[a] Replacement of O vs N ligand.

effects is smaller.[26] There, a Cu–O–Cu′ variation of 1° leads to a change of the antiferromagnetic spin coupling of 60–90 cm^{-1}.[36]

The change from antiferromagnetic to ferromagnetic exchange coupling can be understood when the energies of the SOMO's obtained from the open-shell SCF calculation and their atomic orbital contributions are examined. Figure 7 shows a schematic representation of the symmetric and antisymmetric SOMO's σ_g and σ_u transforming as A′ and A″ of the point group C_s. Their energy difference

$$\Delta\epsilon = \epsilon(\sigma_u) - \epsilon(\sigma_g) \qquad (4)$$

as function of φ_{AB}, r_{Cu-O}, and O vs N is presented in Figure 8. With an increased folding of the copper coordination planes $\Delta\epsilon$ decreases and near $\varphi_{AB} = 90°$ both SOMO's are degenerate. This effect explains the ferromagnetic coupling for folded structures since to a first approximation, $2J_{calcd}(\Delta\epsilon \to 0) \approx 2K_{ab}$. K_{ab} is the two-electron quantum-mechanical exchange integral of the localized magnetic orbitals a and b and is associated with the parallel alignment of the two interacting spins. In case of planar geometry, second and higher order terms arise in the CI treatment and compensate the positive terms because they favor antiparallel alignment. These results can be interpreted in the same way by using the Hay–Thibeault–Hoffmann model[37] or the model of Kahn and Briat.[38] An extended Hückel study of the folding of the CuO_2 planes in a Cu_2O_2 system led to comparable results as

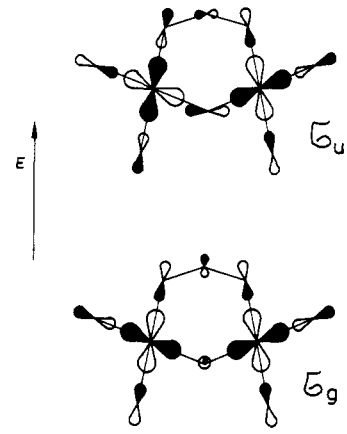

Figure 7. Schematic representation of the singly occupied molecular orbitals σ_g and σ_u in M1 as obtained from the open-shell SCF calculation.

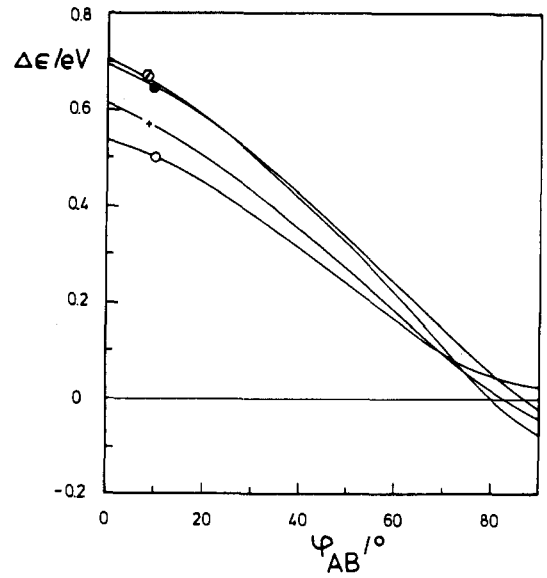

Figure 8. Energy difference $\Delta\epsilon$ between the SOMO's σ_g and σ_u (eq 4). The symbols for different Cu1–O1 distances and the replacement O- vs N-donors agree with those of Figure 6.

presented here.[39] This emphasizes that the folding of the copper coordination planes is the decisive structural parameter for the exchange coupling in the Cu(II)–RO/RCO_2–Cu(II) unit.

The $\Delta\epsilon(\varphi_{AB}, r_{Cu-O})$ function itself can be understood by looking at the atomic orbitals which form the SOMO's σ_g and σ_u. The copper atoms contribute nearly independently from the degree of the folding with $d_{x^{*2}-y^{*2}}$ orbitals point toward the square planar ligand arrangement. x^*, y^*, and z^* refer to a local coordination system in which Cu1 defines the origin, Cu1–O1 defines the x^* axis, and Cu1, O1, and O2 define the x^*y^* plane (Figure 5). Nonbridging donor atoms and the carboxylato oxygen O2 contribute p orbitals which overlap with the copper d orbital in a σ-antibonding fashion. The AO contributions of bridging atoms positioned on the mirror plane, O1 and C2, are restricted for symmetry reasons. Hence, they are represented in σ_g by a linear combination of s, p_y, and p_z but in σ_u only by p_x. As the O1 coefficients are greater than the C2 coefficients, it can be concluded that the electronic and structural properties of the alkoxo bridge determine the exchange coupling in the mixed-bridged unit. The variation of $\Delta\epsilon$ with an increased folding can be understood as followed: $\epsilon(\sigma_g)$ decreases strongly with greater φ_{AB} angles as the overlap $\langle p_x(O1)|d_{x^{*2}-y^{*2}}(Cu1)\rangle$ is strongly influenced. The dominating s character of O1 in σ_u leads to a minor influence on $\epsilon(\sigma_u)$ as $\langle s(O1)|d_{x^{*2}-y^{*2}}(Cu1)\rangle$ does not depend

(36) Haase, W.; Gehring, S. In ref 32.
(37) Hay, P. J.; Thibeault, J. C.; Hoffmann, R. *J. Am. Chem. Soc.* **1975**, *97*, 4884.
(38) Kahn, O. *Angew. Chem.* **1985**, *97*, 837 and references therein.
(39) Charlot, M. F.; Jeannin, S.; Jeannin, Y.; Kahn, O.; Lucrece-Abaul, J.; Martin-Frere, J. *Inorg. Chem.* **1979**, *18*, 1675.

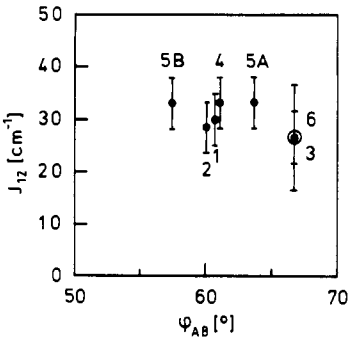

Figure 9. Experimental ferromagnetic coupling constants J_{12} (with error estimates) in the trinuclear copper(II) complexes **1–6** vs dihedral angle φ_{AB}.

on φ_{AB} and Cu1–O1–Cu1′, respectively. Both effects result in a decrease of $\Delta\epsilon$ with increased folding.

The knowledge of the atomic orbitals involved in the exchange coupling allows a discussion of possible superexchange pathways. The atomic p-orbital contributions of O1 change with φ_{AB}. Expressed in terms of the asterisked local coordinate system, O1 contributes with p_{x^*} and p_{y^*} when the planar geometry with $\varphi_{AB} \neq 0°$ is realized. The result is a nonzero copper–oxygen overlap, $\langle d_{x^{*2}-y^{*2}}(Cu1)|p_{x^*},p_{y^*}(O1)\rangle \neq 0$. This may explain the antiferromagnetic coupling on an atomic orbital basis in a rough approximation. When the folding is increased, the p_{z^*} coefficient of O1 dominates. Then the orthogonality of the magnetic orbitals can be explained with the zero overlap $\langle d_{x^{*2}-y^{*2}}(Cu1)|p_{z^*}(O1)\rangle$. The pathways discussed for the asymmetric unit of a trinuclear model compound derived from **1**[6] hold also for the symmetric model M1.

A comparison between the experimental and theoretical results will conclude this section. The experimental coupling constants J_{12} obtained for the trinuclear compounds **1–6** from magnetic susceptibility measurements are presented in Figure 9 as function of φ_{AB}. These data agree with the theoretical result of a ferromagnetic spin coupling and the magneto–structural correlation $J_{calcd} \approx$ constant in the range $50° \leq \varphi_{AB} \leq 70°$. An exact numerical agreement between the experimental J_{12} and the theoretical $2J_{calcd}$ cannot be expected as the calculations have been performed for dimeric model molecules and the experimental data have been obtained from trinuclear systems with a different spin multiplet scheme. As discussed previously,[26,34,36] the basis results of these calculations are the magneto–structural correlations.

The $2J_{calcd}(\varphi_{AB}, r_{Cu-O})$ functions can also be proved by looking at dinuclear oxo/carboxylato-bridged copper(II) complexes. The five molecules in consideration show experimental $2J$ values of -170 ± 10 cm^{-1} at $\varphi_{AB} = 5–19°$ and square planar CuL_4 chromophores at both metal sites.[40] These data show that the magneto–structural correlations presented in Figure 6 are also valid for planar structures with antiferromagnetic exchange coupling.

Acknowledgment. This work was gratefully supported by the Deutsche Forschungsgemeinschaft, Bonn-Bad Godesberg. We thank Dr. E. Bill, Medizinische Universität Lübeck, for helpful discussions and the recording of EPR spectra.

Supplementary Material Available: Listings of anisotropic thermal parameters and hydrogen atom coordinates (Tables S2 and S6), experimental and calculated magnetic susceptibilities (Tables S3 and S7), and intensity collection parameters (Tables S4 and S8) (12 pages). Ordering information is given on any current masthead page.

(40) (a) Nishida, Y.; Takeuchi, M.; Takahashi, K.; Kida, S. *Chem. Lett.* **1983**, 1815. (b) Nishida, Y.; Takeuchi, M.; Takahashi, K.; Kida, S. *Chem. Lett.* **1985**, 631. (c) Nishida, Y.; Kida, S. *J. Chem. Soc., Dalton Trans.* **1986**, 2633. (d) Mazurek, W.; Kennedy, B. J.; Murray, K. S.; O'Connor, M. J.; Rodgers, J. R.; Snow, M. R.; Wedd, A. G.; Zwack, P. R. *Inorg. Chem.* **1985**, *24*, 3258. (e) Butcher, R. J.; Diven, G.; Erickson, G.; Mockler, G. M.; Sinn, E. *Inorg. Chim. Acta* **1986**, *123*, L17. (f) For further oxo/carboxylato-bridged dinuclear copper(II) complexes and a more detailed discussion, see ref 17.